

Impact of Plaque Components on Fractional Flow Reserve-Derived Computed Tomography in Severe Coronary Stenosis

Ciddi Koroner Stenozda Plak İçeriğinin Fraksiyonel Akım Rezervinden Derive Edilmiş Bilgisayarlı Tomografi Üzerindeki Etkisi

ABSTRACT

Fractional flow reserve derived from computed tomography decreases across severe coronary stenosis. The diagnostic accuracy of fractional flow reserve-derived computed tomography is high for severe coronary stenosis. In this report, we present a case of no significant fractional flow reserve-derived computed tomography changes even in severe coronary stenosis. A 75-year-old man showed severe stenosis (85% diameter stenosis) in the distal segment of the right coronary artery on both computed tomography angiography and invasive coronary angiography. However, fractional flow reserve-derived from computed tomography showed no significant changes from the proximal (0.97) to the distal (0.95) segments despite the presence of severe stenotic lesion. This patient had different features including the presence of a large acute marginal branch and significantly lower plaque components in the stenotic lesion compared with another patient who had coronary stenosis in the same segment. A large bifurcation branch and/or proportion of plaque components can affect fractional flow reserve-derived from computed tomography hemodynamics.

Keywords: Computed tomography, fractional flow reserve, imaging

ÖZET

Bilgisayarlı tomografi kaynaklı fraksiyonel akım rezervi (FFR-BT), ciddi koroner stenozlarda azalır. FFR-BT'nin tanınal doğruluğu ciddi koroner stenoz için yüksektir. Bu olgu bildirisinde, ciddi koroner stenozda bile anlamlı FFR-BT değişikliği olmayan bir hasta sunuldu. 75 yaşında erkek hastada, hem BT anjiyografi hem de invaziv koroner anjiyografide, sağ koroner arterin distal segmentinde ciddi stenoz (%85 çapında darlık) görüldü. Bununla birlikte, FFR-BT'de bu ciddi stenotik lezyonda bile proksimalden (0.97) distal segmentlere (0.95) önemli bir değişiklik görülmedi. Bu hastada, aynı segmentte ciddi darlığı olan başka bir hasta ile karşılaştırıldığında, geniş bir akut marjinal dalın varlığı ve stenotik lezyonda önemli oranda daha az plak içeriği gibi farklı özellikler mevcuttu. Geniş bir bifurkasyon dalı varlığı ve/veya plak içeriğinin oranı, FFR-BT hemodinamiğini etkileyebilir.

Anahtar Kelimeler: Bilgisayarlı tomografi, görüntüleme, fraksiyonel akım rezervi

It is well known that fractional flow reserve-derived from computed tomography (FFR_{CT}) is affected by various factors such as vessel morphology,¹ plaque characteristics,¹ bifurcation angle,² lumen volume (LV) mass,³ bifurcation angle, and branches.^{4,5} To improve the diagnostic accuracy of FFR_{CT}, factors affecting FFR_{CT} have been investigated. Previous studies investigated FFR_{CT} based on each entire vessel, but not on the stenotic lesion alone. To our knowledge, this is the first report of the following: (1) no significant changes across the severe stenotic lesion, (2) investigation of the relationship between FFR_{CT} dynamics and lesion-specific morphology in the severe stenotic lesion. Herein, we present a 75-year-old man who presented no significant FFR_{CT} changes even in severe stenosis. Moreover, the present case was compared with severe coronary stenosis in the same segment.

CASE REPORT OLGU SUNUMU

Toshimitsu Tsugu¹ 

Kaoru Tanaka¹ 

Yuji Nagatomo² 

Michel De Maeseneer¹ 

Johan De Mey¹ 

¹Department of Radiology, Universitair Ziekenhuis Brussel, Brussels, Belgium

²Department of Cardiology, National Defense Medical College Hospital, Tokorozawa, Japan

Corresponding author:

Toshimitsu Tsugu

✉ tsugu917@gmail.com

Received: September 26, 2022

Accepted: December 12, 2022

Cite this article as: Tsugu T, Tanaka K, Nagatomo Y, De Maeseneer M, De Mey J. Impact of plaque components on fractional flow reserve-derived computed tomography in severe coronary stenosis. *Türk Kardiyol Dern Ars.* 2023;51(5):356-360.

DOI:10.5543/tkda.2022.57522



Available online at archivestsc.com.
Content of this journal is licensed under a Creative Commons Attribution - NonCommercial-NoDerivatives 4.0 International License.

Case Reports

A total of 1503 outpatients with suspected coronary artery disease and who had FFR_{CT} analysis were examined between January 2017 and May 2022. Only 1 patient (Case 1) showed no significant FFR_{CT} changes across the severe coronary stenosis in the distal segment of the RCA. To further investigate the cause of this phenomenon, Case 2 with stenotic lesions at the same site as Case 1 was selected from all eligible patients and vessel characteristics were compared.

All coronary computed tomography angiography (CCTA) scans were performed on a GE Revolution scanner (GE, Milwaukee, USA). Beta-blockers were administered when necessary to obtain a heart rate of < 60 beats/min. Sublingual nitrates (2 sprays of 0.8 mg) were administered before scanning in all patients. Fractional flow reserve-derived from computed tomography was analyzed using HeartFlow Inc. (Redwood City, California, USA). Computational fluid dynamics and blood flow simulations were performed to calculate the FFR_{CT} at any arbitrary point in the coronary artery. $\Delta\text{FFR}_{\text{CT}}$ was defined as the change in FFR_{CT} from the proximal to the distal across the stenotic lesion. Vessel morphology and components were measured using GE AW server 3.2 software (GE Healthcare, Chicago, IL, USA) and Colour Code Plaque (GE Healthcare, Chicago, IL, USA). Vessel components were characterized based on Hounsfield units into low-attenuation plaque (LAP) (< 30 HU), intermediate-attenuation plaque (IAP) (30–150 HU), and calcified plaque (CP) (> 150 HU).⁶ Fractional flow reserve-derived from computed tomography (HeartFlow Inc., Redwood City, CA, USA) was calculated based on a 3-dimensional anatomical model synthesized from CT angiographic data. The volume of the myocardium extracted from the image data was multiplied by an average value of myocardial tissue density (1.05 g/mL) to calculate LV myocardial mass. Lumen volume mass index was calculated by dividing the LV mass by the body surface area.³

Case 1

A 75-year-old man was admitted with chest discomfort at exertion. Coronary computed tomography angiography revealed severe coronary stenosis (85% diameter stenosis) (Figure 1A–C, dotted line) around the divergence of the large acute marginal branch in the distal segment of the right coronary artery (RCA). The stenotic lesion was focal (17.5 mm) and consisted of lumen volume 141.3 mm³, LAP 0 mm³, IAP 1.7 mm³, and CP 0 mm³ (Table 1, Figure 1C). Plaque components in the stenotic lesion were only 1.2% (Table 2 and Figure 2). FFR_{CT} at the RCA ostium was 1.00 and gradually decreased to 0.91 at the distal end of the RCA. No steep FFR_{CT} decline ($\Delta\text{FFR}_{\text{CT}}$: 0.02) was observed at the stenotic lesion (Figures 1D and 1E). Invasive coronary

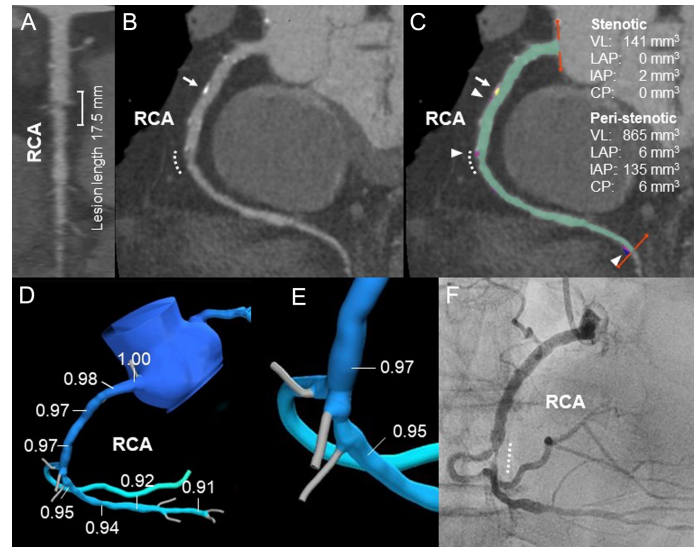


Figure 1. Case 1. Coronary computed tomography angiography (A–C): (A) Stretched multiplanar reformation. (B) Curved multiplanar reformation. (C) Vessel components. Green, VL; red, IAP; and yellow, CP. (D and E) Fractional flow reserve-derived computed tomography. $\Delta\text{FFR}_{\text{CT}}$ is the difference between the proximal and the distal segment of the stenotic lesion. (F) Invasive coronary angiography. The dotted line, arrowhead, and arrow indicate stenotic lesion, IAP, and CP, respectively. CP, calcified plaque; CCTA, coronary computed tomography angiography; FFR_{CT}, fractional flow reserve-derived computed tomography; IAP, intermediate-attenuation plaque; LAP, low-attenuation plaque; RCA, right coronary artery; VL, vessel lumen.

Table 1. Vessel Morphology and Components at the Stenotic Lesion and Peri-stenotic Lesion

	Case 1	Case 2
<i>Total vessel</i>		
Vessel length (mm)	122.1	117.7
Lumen volume (mm ³)	1006.5	728.8
LAP volume (mm ³)	6.4	31.6
IAP volume (mm ³)	36.3	216.3
CP volume (mm ³)	5.8	13.3
<i>Stenotic lesion</i>		
Vessel length (mm)	17.5	17.5
Lumen volume (mm ³)	141.3	69.6
LAP volume (mm ³)	0	22.0
IAP volume (mm ³)	1.7	73.9
CP volume (mm ³)	0	0.1
<i>Peri-stenotic lesion</i>		
Vessel length (mm)	104.6	100.2
Lumen volume (mm ³)	865.2	659.2
LAP volume (mm ³)	6.4	9.6
IAP volume (mm ³)	34.6	142.4
CP volume (mm ³)	5.8	13.2

CP, calcified plaque; IAP, intermediate-attenuation plaque; LAP, low-attenuation plaque.

ABBREVIATIONS

CCTA	Coronary computed tomography angiography
CFD	Computational fluid dynamics
CP	Calcified plaque
FFR _{CT}	Flow reserve-derived computed tomography
LAP	Low-attenuation plaque
LV	Lumen volume
RCA	Right coronary artery

angiography showed severe coronary stenosis (dotted line) in the distal segment of the RCA (Figure 1F).

Case 2

A 71-year-old woman was admitted with chest discomfort at exertion. Coronary computed tomography angiography revealed severe coronary stenosis (95% diameter stenosis) (Figures 3A-C, dotted line) in the distal segment of the RCA. The stenotic lesion was focal (17.5 mm) and consisted of lumen volume 69.6 mm³, LAP 22.0 mm³, IAP 73.9 mm³, and CP 0.1 mm³ (Table 1, Figure 3C). Plaque components of the stenotic lesion were 58.0% (Table 2 and Figure 2). Fractional flow reserve-derived from computed tomography at the RCA ostium was 1.00 and a decline during the stenotic lesion, resulting in 0.56 at the distal end of the RCA ($\Delta\text{FFR}_{\text{CT}}$: 0.38) (Figures 3D and 3E). Invasive coronary angiography showed severe coronary stenosis (dotted line) in the distal segment of the RCA (Figure 3F).

Discussion

It is well known that FFR_{CT} dynamics depend on not only stenotic severity but also the site of the stenotic lesion. The present study investigated the impact of vessel morphology (vessel length, lumen volume) and plaque components in stenotic and peri-stenotic lesions with severe coronary stenosis on FFR_{CT} dynamics. Fractional flow reserve-derived from computed tomography dynamics differed significantly between Case 1 and Case 2, despite the same stenotic severity in the same segment. The differences between Case 1 and Case 2 were the presence of the large acute marginal branch and the lack of plaque components in the stenotic lesion (Table 3). The following possibilities could be considered as the mechanisms that caused differences in FFR_{CT} dynamics. First, the presence of the bifurcation branch

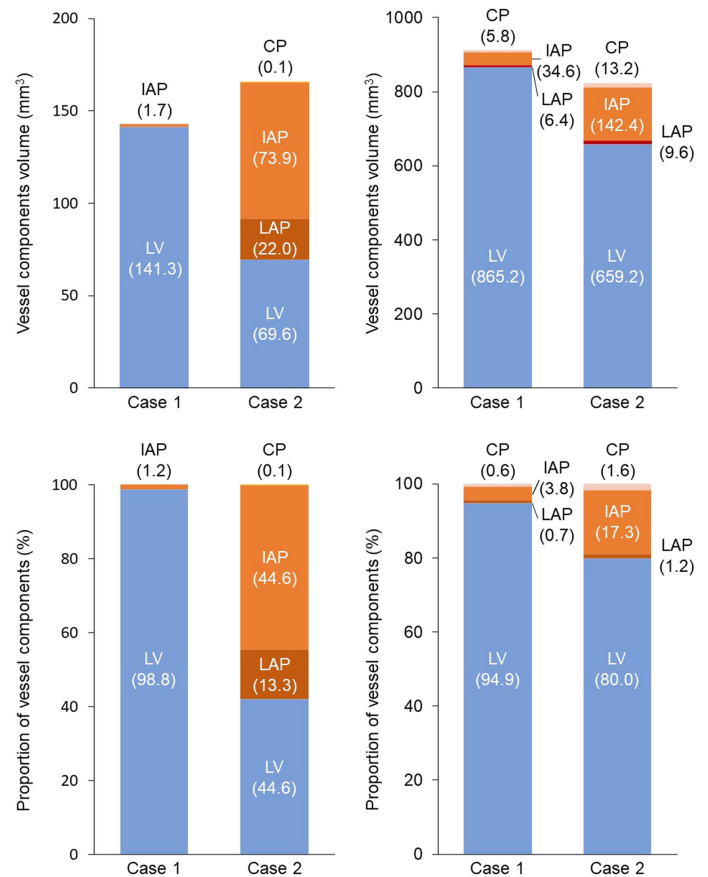


Figure 2. (A) Vessel components volume in the stenotic lesion. (B) Vessel components volume in peri-stenotic lesions. (C) Proportion of vessel components in stenotic lesion. (D) Proportion of vessel components in peri-stenotic lesions. CP, calcified plaque; IAP, intermediate-attenuation plaque; LAP, low-attenuation plaque; LV, lumen volume.

Table 2. The Proportion of Vessel Components at the Stenotic Lesion and Peri-stenotic Lesion

	Case 1	Case 2
<i>Total vessel</i>		
Lumen volume (%)	95.4	73.6
LAP volume (%)	0.6	3.2
IAP volume (%)	3.4	21.8
CP volume (%)	0.5	1.3
<i>Stenotic lesion</i>		
Lumen volume (%)	98.8	42.0
LAP volume (%)	0	13.3
IAP volume (%)	1.2	44.6
CP volume (%)	0	0.1
<i>Peri-stenotic lesion</i>		
Lumen volume (%)	94.9	80.0
LAP volume (%)	0.7	1.2
IAP volume (%)	3.8	17.3
CP volume (%)	0.6	1.6

CP, calcified plaque; IAP, intermediate-attenuation plaque; LAP, low-attenuation plaque.

may cause turbulent flow after the stenotic lesion, consuming thermal energy and consequently affecting FFR_{CT} hemodynamics.^{4,5} In both Case 1 and Case 2, the stenotic lesions were located at the distal of bifurcation branch, thus the differences in the effects of branch was not significant. Second, plaque components of the stenotic lesion and peri-stenotic lesion in Case 1 were markedly smaller than those in Case 2 (Case 1 vs. Case 2; stenotic, 1.2% vs. 58.0%; peri-stenotic, 5.1% vs. 20.0%) (Table 2 and Figure 2). Deposition of plaque components could lead to impaired functional vasodilatory capacity due to oxidative stress and inflammation (Figure 4A).^{7,8} The inhomogeneous contrast of plaque components between stenotic and peri-stenotic generated a pressure gradient during maximal hyperemia, contributing to differences of FFR_{CT} values (Figure 4B). Collectively, the extremely small amount of plaque components assessed by CCTA in the stenotic lesion may accelerate total vessel dilatation, including the stenotic lesion, during maximal hyperemia. Consequently, a lack of pressure gradient between the stenotic and per-stenotic lesions may be responsible for the reduced changes in FFR_{CT}. This study highlighted the large acute marginal branch and the lack of plaque components in the stenotic lesion may contribute to the atypical FFR_{CT} hemodynamics. This report

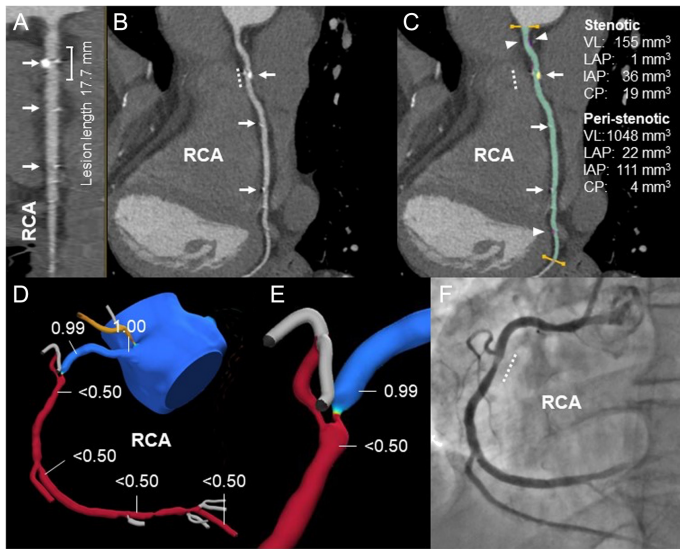


Figure 3. Case 2. The dotted line, arrowhead, and arrow indicate stenotic lesion, IAP, and CP, respectively. CP, calcified plaque; CTA, computed tomography angiography; FFR_{CT}, fractional flow reserve-derived computed tomography; IAP, intermediate-attenuation plaque; LAP, low-attenuation plaque; RCA, right coronary artery; VL, vessel lumen.

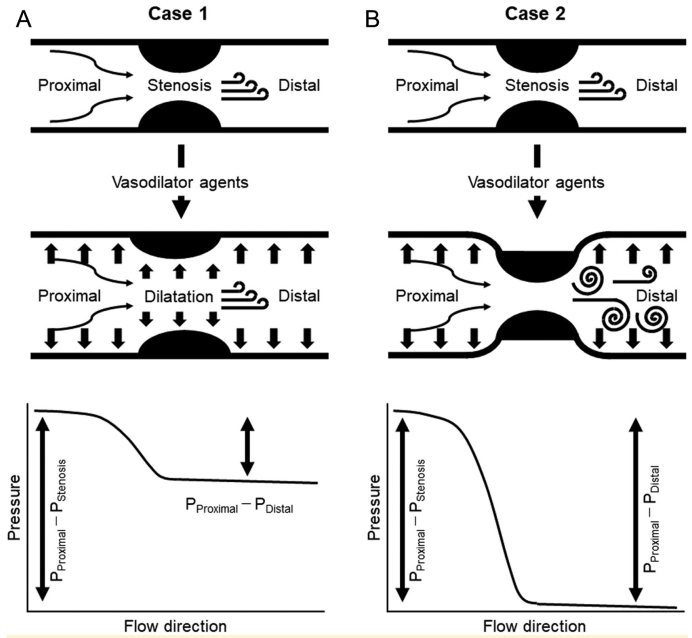


Figure 4. Schema of the effects of different components of the stenotic lesions on FFR_{CT} dynamics. (A) Case 1. (B) Case 2. FFR_{CT}, fractional flow reserve-derived computed tomography.

has some limitations. First, this phenomenon was observed in only 1 case among enrolled 1503 patients. It was still unclear whether the cause of this phenomenon (no significant FFR_{CT} changes even in severe coronary stenosis) was due to the difference in plaque volume between stenotic and peri-stenotic lesions or a purely technical error based on computational fluid dynamics (CFD) analysis. Fractional flow reserve-derived from computed tomography values are calculated by blood flow

simulations and CFD. Computational fluid dynamics is a simulation method that calculates approximate solutions based on discretizing the Navier–Stokes equation which described the motion of viscous fluid substances. Computational fluid dynamics is calculated based on the results of various hypotheses and models, thus CFD has the potential to cause errors. The second limitation is the lack of enforcement of invasive FFR. Nevertheless, previous studies have shown that FFR_{CT} can be an alternative test for invasive FFR due to the high concordance between FFR_{CT} and invasive FFR.¹⁰⁻¹² Third, it has been believed that non-calcified plaque and thrombus components can be distinguished by HU values. However, as reported by Niesten et al.⁹ the composition of thrombus varies widely, including, fibrin and red blood cells. Thrombus abundant in fibrin and platelet exhibit a low level of HU values, thus distinguishing between non-calcified plaque and thrombus could have been difficult with CCTA alone. Thrombus components might be contaminated in the non-calcified plaque components. In Case 1, stenotic lesion with vulnerable components of thrombus and non-calcified plaque may have the potential to obtain temporary vasodilation during the maximal hyperemia, resulting in the disappearance of pressure gradient before and after stenotic lesions. In this report, our proposed mechanism mentioned above cannot be confirmed by further evidence and is still hypothesis-generating. Further accumulation of similar cases and their detailed analysis could confirm our hypothesis. It has been believed that FFR_{CT} drops downward significantly across severely stenotic lesions. However, we reported no significant changes in FFR_{CT} across the severe stenotic lesion. Vessel morphology and plaque components should be considered when interpreting FFR_{CT}. may provide useful information for FFR_{CT} interpretation. These findings may have the potential to assess an accurate diagnosis of FFR_{CT}.

Table 3. Characteristics of the Patient Population

	Case 1	Case 2
Age (years)	75	71
Gender	Man	Woman
Height (cm)	178	158
Body weight (kg)	87	62
Body surface area (kg/m ²)	2.1	1.6
Body mass index (kg/m ²)	27	25
Heart rate (beats/min)	60	60
Atrial fibrillation	-	-
Hypertension	+	+
Dyslipidemia	-	-
Diabetes	-	-
Current smoking	-	+
Left ventricular mass (g)	125	80
Left ventricular mass index (g/m ²)	61	49

CP, calcified plaque; IAP, intermediate-attenuation plaque; LAP, low-attenuation plaque.

Conclusion

The presence of large bifurcation and the absence of vessel plaque components in the stenotic lesion may have the potential to affect FFR_{CT} hemodynamics.

Ethics Committee Approval: Ethical committee approval was received from the Ethics Committee of Universitair Ziekenhuis Brussel, (Approval No: B.U.N. 143202000302).

Informed Consent: Written informed consent was obtained from the patients for the publication of the case report and the accompanying images.

Peer Review: Externally peer-reviewed.

Author Contributions: Conception – T.T.; Design – T.T.; Supervision – K.T., Y.N., M.D.M., J.D.M.; Data collection – T.T.; Writing – T.T., Y.N.; Critical Review – T.T., K.T.

Declaration of Interests: The authors declare that they have no competing interests.

Funding: The authors declare that this study received no financial support.

References

1. Tsugu T, Tanaka K, Belsack D, et al. Impact of vascular morphology and plaque characteristics on computed tomography derived fractional flow reserve in early stage coronary artery disease. *Int J Cardiol.* 2021;343:187–193. [\[CrossRef\]](#)
2. Tsugu T, Tanaka K, Nagatomo Y, et al. Impact of coronary bifurcation angle on computed tomography derived fractional flow reserve in coronary vessels with no apparent coronary artery disease. *Eur Radiol.* 2023;33(2):1277–1285. [\[CrossRef\]](#)
3. Tsugu T, Tanaka K, Belsack D, et al. Effects of left ventricular mass on computed tomography derived fractional flow reserve in significant obstructive coronary artery disease. *Int J Cardiol.* 2022;355:59–64. [\[CrossRef\]](#)
4. Tsugu T, Tanaka K. Differences in fractional flow reserve derived from coronary computed tomography angiography according to coronary artery bifurcation angle. *Turk Kardiyol Dern Ars.* 2022;50(1):83–84. [\[CrossRef\]](#)
5. Tsugu T, Tanaka K, Nagatomo Y, Belsack D, De Maeseneer M, De Mey J. Paradoxical changes of coronary computed tomography derived fractional flow reserve. *Echocardiography.* 2022;39(2):398–403. [\[CrossRef\]](#)
6. Motoyama S, Sarai M, Harigaya H, et al. Computed tomographic angiography characteristics of atherosclerotic plaques subsequently resulting in acute coronary syndrome. *J Am Coll Cardiol.* 2009;54(1):49–57. [\[CrossRef\]](#)
7. Ahmadi A, Stone GW, Leipsic J, et al. Association of coronary stenosis and plaque morphology with fractional flow reserve and outcomes. *JAMA Cardiol.* 2016;1(3):350–357. [\[CrossRef\]](#)
8. Lavi S, Yang EH, Prasad A, et al. The interaction between coronary endothelial dysfunction, local oxidative stress, and endogenous nitric oxide in humans. *Hypertension.* 2008;51(1):127–133. [\[CrossRef\]](#)
9. Niesten JM, van der Schaaf IC, van Dam L, et al. Histopathologic composition of cerebral thrombi of acute stroke patients is correlated with stroke subtype and thrombus attenuation. *PLOS ONE.* 2014;9(2):e88882. [\[CrossRef\]](#)
10. Koo BK, Erglis A, Doh JH, et al. Diagnosis of ischemia-causing coronary stenoses by noninvasive fractional flow reserve computed from coronary computed tomographic angiograms. Results from the prospective multicenter DISCover-FLOW (Diagnosis of Ischemia-Causing stenoses Obtained via Noninvasive Fractional Flow Reserve) study. *J Am Coll Cardiol.* 2011;58(19):1989–1997. [\[CrossRef\]](#)
11. Douglas PS, Pontone G, Hlatky MA, et al. Clinical outcomes of fractional flow reserve by computed tomographic angiography-guided diagnostic strategies vs. usual care in patients with suspected coronary artery disease: the prospective longitudinal trial of FFR(CT): outcome and resource impacts study. *Eur Heart J.* 2015;36(47):3359–3367. [\[CrossRef\]](#)
12. Min JK, Taylor CA, Achenbach S, et al. Noninvasive fractional flow reserve derived from coronary CT angiography: clinical data and scientific principles. *JACC Cardiovasc Imaging.* 2015;8(10):1209–1222. [\[CrossRef\]](#)